Solar Energy Materials & Solar Cells ▮ (▮▮▮▮) ▮▮▮–▮▮▮

Contents lists available at ScienceDirect

Solar Energy Materials & Solar Cells

journal homepage: www.elsevier.com/locate/solmat

Response to simulated typical daily outdoor irradiation conditions of thin-film silicon-based triple-band-gap, triple-junction solar cells

P. Krishnan [a], J.W.A. Schüttauf [a], C.H.M. van der Werf [a], B. Houshyani Hassanzadeh [b], W.G.J.H.M. van Sark [b], R.E.I. Schropp [a,*]

[a] Nanophotonics—Physics of Devices, Department of Physics and Astronomy, Debye Institute for Nanomaterials Science, Faculty of Science, Utrecht University, P.O. Box 80000, 3508 TA Utrecht, The Netherlands

[b] Department of Chemistry, Science, Technology and Society, Faculty of Science, Utrecht University, Heidelberglaan 2, 3584 CS Utrecht, The Netherlands

ARTICLE INFO

Article history:
Received 15 December 2007
Accepted 16 September 2008

Keywords:
Spectral variation
Thin-film Si solar cells
Triple junction
Nanocrystalline
Current matching
Performance

ABSTRACT

We studied the response to various realistic outdoor conditions of thin-film silicon-based triple-band-gap, triple-junction cells that were made in house. The triple-junction cells consist of a stack of proto-Si:H/proto-SiGe:H/nanocrystalline (nc)-Si:H cells in an n–i–p configuration, fabricated using hot-wire chemical vapour deposition (CVD). Current matching was determined for modeled spectra of four different days of the year that are typical for the northwestern European climate. Spectral modeling was based on measured irradiation data. The results showed that on a clear day in June, when the actual spectrum was closest to the reference AM1.5 spectrum, the matching was ideal. As the spectral shape varied during the course of the day with respect to the AM1.5 reference the matching became progressively worse. We found that the top cell (1.8 eV) and bottom cell (1.1 eV) are most sensitive to spectral changes, whereas the middle cell (1.5 eV) is less sensitive. Overall, it was evident that either cloudiness or seasonal variations led to an increase in current mismatch between the cells. If the sub-cells are closely matched, it may even occur that a cell designed to be current limiting no longer fulfills that role.

1. Introduction

Solar cell performance is affected by irradiation intensity, cell temperature, and solar spectral distribution, in order of decreasing importance. In performance models usually a spectral mismatch factor is included, which represents an aggregated annual energy loss of several percent. This is in contrast to variations in spectral distributions due to varying meteorological conditions, besides variations induced by location, time, and season, see e.g., Ref. [1]. The magnitude of solar spectral effects on different photovoltaic (PV) technologies depends on the band gap of the cells, i.e., solar cells made from materials with a larger band gap lead to a larger spectral effect [2]. Therefore, a PV device with a narrow spectral response such as amorphous silicon (a-Si) is more sensitive to changes in the spectral composition of irradiation, compared to a wider spectral response device such as crystalline silicon (c-Si).

Multi-junction solar cells are optimized using the standard Air Mass 1.5 (AM1.5) spectrum, as its use is prescribed in the present measurement standard test conditions (STC). Current matching is essential in these devices, and spectral response optimization of each cell in the device is performed on the basis of this standard spectrum. As the spectral distribution varies from the standard, the currents in the various cells in the device vary as well, leading to increased spectral and current mismatch and concomitant loss of power. Hirata and Tani [3] and Hirata et al. [4] reported varying performance of an a-Si tandem module by direct measurement of the module performance; a difference of −6% to +14% in output of the module was found with respect to calculated performance using the standard AM1.5 spectrum, depending on different seasons. Minemoto et al. [5] showed that a-Si:H/μc-Si:H 'micro-morph' modules are spectrally more sensitive than c-Si modules. Detailed results on the spectral variation in the Israeli desert and its effect on the outdoor performance of PV modules have been published by Berman et al. [6]. Gottschalg et al. [7] have shown that the useful fraction (UF), defined as the ratio of observed radiation in the useful spectral range for the PV device studied to the global radiation, for different thin-film devices, varies considerably. Clearly the higher the UF, the more energy will be produced, and UF is always lower than 1. The UF of CIGS cells varied between +1.5% and −1.5% compared to the annual average, while the UF of CdTe cells varied between +4% and −6%. For a-Si:H, the most strongly affected device, the variation is between +6% and −9% [7]. The geography of the testing is a significant variable. A similar study in Japan showed a variation up to 14% for a-Si:H cells and 5% for polycrystalline-Si (poly-Si) cells [3,4].

* Corresponding author.
E-mail address: r.e.i.schropp@uu.nl (R.E.I. Schropp).

0927-0248/$ - see front matter © 2008 Elsevier B.V. All rights reserved.
doi:10.1016/j.solmat.2008.09.031

The present paper aims to assess the effect of spectral variation on silicon thin-film triple proto-Si:H/proto-SiGe:H/nanocrystalline (nc)-Si:H cells in an n–i–p configuration, fabricated using in-house hot-wire chemical vapour deposition (HWCVD) equipment. The effect is studied quantitatively by looking at the current matching of the triple cell as the daily spectrum changes. To this end, spectra are modeled based on measured irradiation data using the spectrum simulation model SEDES2 [8]. The band gap of the three layers is about 1.8, 1.5, and 1.1, from top to bottom. High-energy light of short wavelengths in the ultraviolet and blue regime (about 350–450 nm) is absorbed in the top cell of the triple structure. Green light at wavelengths of 500–600 nm is absorbed in the middle cell. Lower-energy light of longer wavelengths in the red and infrared regime (800–1000 nm) is absorbed in the bottom cell. The cell output currents are matched, and the cell with the lowest current is the *current-limiting* cell. Changes in the incident spectrum can alter the output of each sub-cell. For example, a higher intensity in the blue wavelength regime causes the top cell to have a higher output than the other cells. This is the challenge that is posed by spectral variation—how to design cells such that they provide optimum matching under a wide range of conditions?

2. Experimental method

2.1. Solar cells

At Utrecht University (UU), several proto-Si:H/proto-SiGe:H/nc-Si:H triple cells were fabricated. The a-Si:H and nc-Si:H layers were made using HWCVD and the a-SiGe:H and doped layers were made using plasma-enhanced CVD. All cells have a transparent conductive oxide (TCO) made out of indium tin oxide (ITO); 80 nm thickness was determined with quarter wavelength interference theory to provide the maximum performance in the range of 550–600 nm, which is the region of the standard spectrum with the highest intensity. Gold contacts were deposited on top of the ITO in 'V' and 'Christmas tree' shapes. Fig. 1 shows a triple-cell sample. Each square is a $4 \times 4\,mm^2$ solar cell with a gold contact. The cells have a transparent back reflector (TBR) made out of Ag/ZnO with a thickness of 100 nm to optimally reflect light in the range of 700–1000 nm [9]. Details of each sub-cell are provided in Table 1.

Two triple cells were used: a well-matched and a poorly matched cell. The current matching was determined under AM1.5 conditions. The normalized current densities of the cells are shown in Table 2. The lowest current was set to 1. These results were obtained through spectral response measurements. It can be seen that in the well-matched cell, the maximum variation of current between the cells is about 11%. By contrast, the current varies by as much as 45% in the poorly matched cell.

One of the drawbacks of the UF method is that it is complicated to study multi-junction devices. Each sub-cell has a different spectral response, which overlaps with that of its neighbours. So it is difficult to define boundaries of spectral range for each sub-cell. Therefore, the UF method was not employed. Instead, the average photon energy (APE) was used. APE is defined as the ratio of total irradiance in the spectrum to total photon flux density in a particular spectral range [5,10]. It provides information about the energy content of the spectrum at each wavelength.

2.2. Spectral data simulation

Solar spectral data are not available in most countries. Therefore we modelled the spectra by employing the SEDES2 spectral model [8]. This model is an extension of SPCTRAL2 [11], which is able to model clear-sky spectra. SEDES2 includes modelling of spectra for cloudy skies, and was updated recently [12]. Required model inputs are total, diffuse and direct irradiance, ambient temperature, pressure, and relative humidity, on any time base. The spectra are calculated in the wavelength range of 300–1400 nm with a step size of 10 nm.

Since March 2005, the Royal Netherlands Meteorological Institute (KNMI) has established its own irradiance measurement station, which continuously records the total, diffuse, and direct irradiance every minute at geographical location of 51.971°N, 4.927°E in Cabauw, a village close to the city of Utrecht. It is part of the Baseline Surface Radiation Network (BSRN) [13]. The data are used in order to derive minutely simulated solar spectrum for a 1-year period from March 1st, 2005 to February 28th, 2006, constituting a full year. Ambient temperature, relative humidity, and pressure were measured on a site near (<100 m) the irradiance measurement set-up. Spectra are calculated by SEDES2 for a 37°-tilted surface directed towards the south. Irradiances less than $10\,W/m^2$ were ignored. We can thus compare the spectra with the ASTM AM1.5G standard [14]. More details are given in Refs. [15,16], in which the spectral effects on amorphous and c-Si solar cells are also discussed as measured on a site near the irradiance measurement set-up.

In the present study, the global intensity for wavelengths between 350 and 1050 nm was used for four typical days to reflect summer and winter days: one clear and one cloudy day in June 2005, and one clear and one cloudy day in December 2005. The data was averaged for each illuminated hour of the day and reported at half-past each hour. In the winter, there were five such data columns for the hours between 0900 and 1500 h. In the summer, there were 12 data columns for the hours between 0600

Table 1
Composition and thickness of each layer of the triple cell's sub-cells

Layer	Top cell	Middle cell	Bottom cell
n	a-Si:H, 5 nm+μc-Si:H, 27 nm	μc-Si:H, 30 nm	μc-Si:H, 30 nm
i	a-Si:H, 180 nm	a-SiGe:H, 250 nm	μc-Si:H, 1700 nm
p	a-Si:H, 23 nm	a-Si:H, 23 nm	a-Si:H, 23 nm

Table 2
Normalized initial sub-cell current densities of the triple-junction cells, and absolute total-cell current

Cell	Top	Middle	Bottom	J_{sc} (mA/cm^2)
Well-matched cell	1.11	1.00	1.04	8.0
Poorly matched cell	1.45	1.00	1.29	8.4

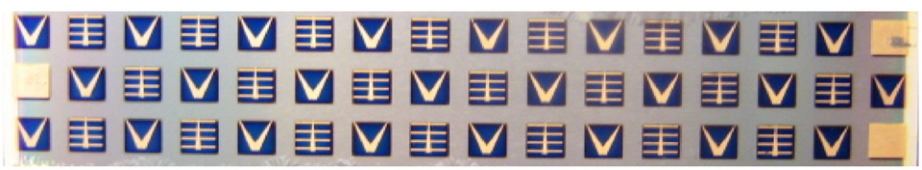

Fig. 1. Triple-cell image showing $4 \times 4\,mm^2$ cells with gold contacts in both V and 'Christmas tree' shapes.

Please cite this article as: P. Krishnan, et al., Sol. Energy Mater. Sol. Cells (2008), doi:10.1016/j.solmat.2008.09.031

and 1800 h. All times were based on true solar time (TST), meaning that at noon, the sun was at its highest elevation. Fig. 2 shows the average spectrum for each day and the AM1.5 spectrum for comparison. From top to bottom, the spectra are: the AM1.5 spectrum, clear June day, clear December day, cloudy June day, and cloudy December day. The AM1.5 spectrum was clearly the strongest. The clear day in June had a similar shape to it but was less intense. The clear December day was less strong in the blue wavelengths but was quite similar to the clear day in June in the red-wavelength regime. Both cloudy days were very weak in direct radiation intensity as expected. The cloudy June day somewhat resembled the AM1.5 and clear June day spectrum, being somewhat higher in the blue than red, while the cloudy December day had a fairly constant profile with low intensity throughout.

The matching was determined for each hour by calculating the current density of each sub-cell for the hour's spectral conditions. The following steps were taken:

(1) intensity was integrated over each 10 nm step to find the intensity in W/m^2;
(2) photon flux was calculated by dividing the intensity by the photon energy in eV at that wavelength;
(3) the average of flux multiplied by the measured ECE of each sub-cell returned the sub-cell current density for each wavelength;
(4) the sum of the current density over all wavelengths produced the final current density.

These steps were repeated for each sub-cell. By performing these calculations for different spectral conditions, the matching properties of the cell could be compared. Additionally, the APE for each time step was calculated to find the 'redness' or 'blueness' of the incident light with respect to the AM1.5 APE, which was 1.88 eV. A value greater than the AM1.5 APE would indicate a blue-shifted spectrum (more high-energy photons) and a lower value would indicate a red-shifted spectrum. Since the spectral data were modelled only during the illuminated hours of the day, the APE was calculated only for those periods.

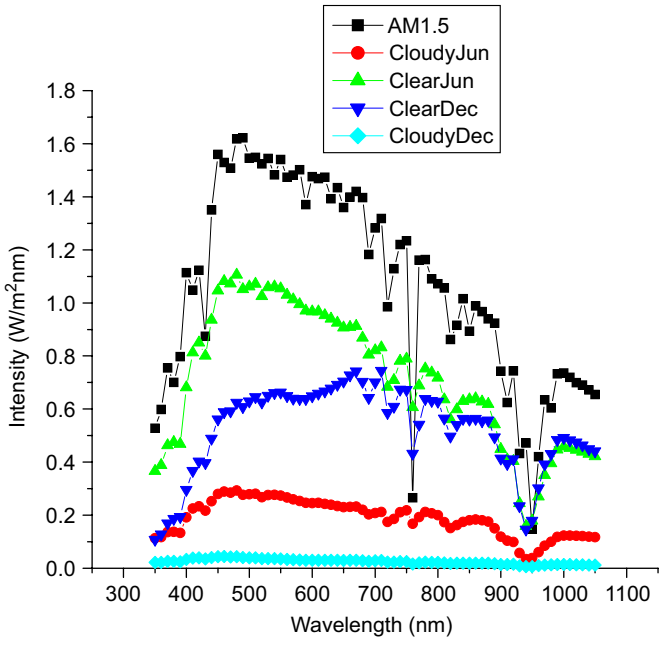

Fig. 2. AM1.5 spectrum and spectra of 4 days in 2005 used in this study.

3. Results and discussion

3.1. June days

The APE of the AM1.5 reference spectrum used was 1.88 eV. The current matching under this spectrum is the reference condition, and the details are given in Table 2. In the following sections, a detailed analysis of each day's spectrum and corresponding current matching is provided.

In the following graphs (Figs. 3–8, 10, 11), the left axis shows normalized current density with the lowest current set to 1. The right axis shows APE in eV. The bottom axis is the measurement time. The stars are APE values, and the squares, circles, and triangles show the top, middle and bottom sub-cell currents, respectively.

The clear June day results for both well-matched and poorly matched cells are shown in Figs. 3 and 4, respectively. The day's APE was 1.89 eV. This is less than a 1% difference compared to the

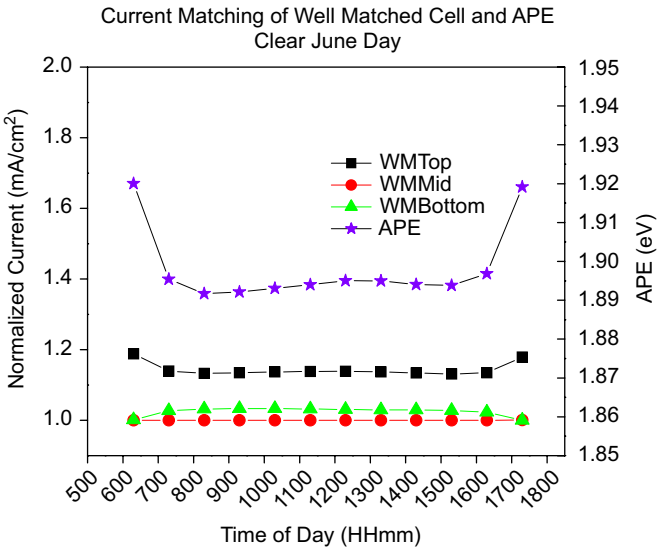

Fig. 3. Well-matched cell's sub-cell currents and APE vs. time of day on the clear June day.

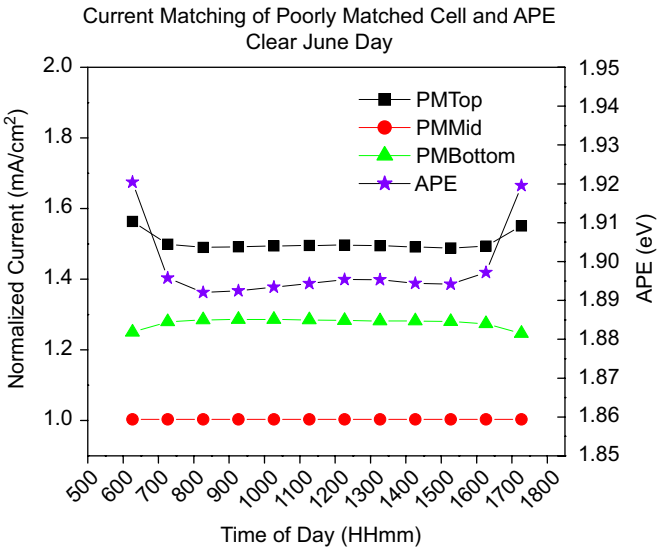

Fig. 4. Poorly matched cell's sub-cell currents and APE vs. time of day on the clear June day.

Please cite this article as: P. Krishnan, et al., Sol. Energy Mater. Sol. Cells (2008), doi:10.1016/j.solmat.2008.09.031

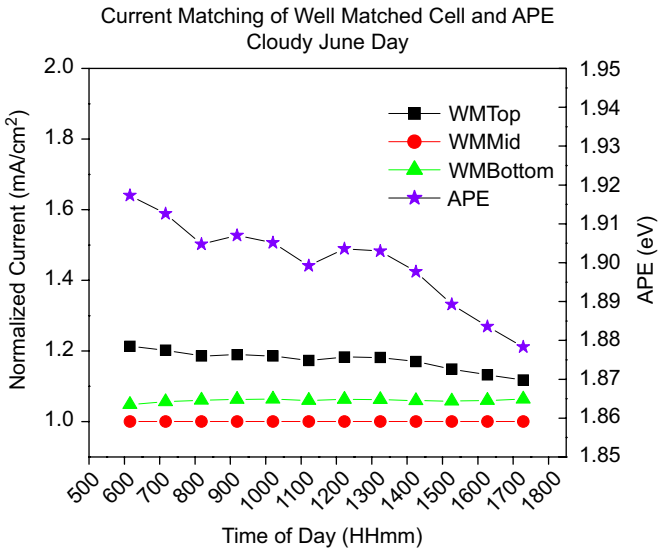

Fig. 5. Well-matched cell's sub-cell currents and APE vs. time of day on the cloudy June day.

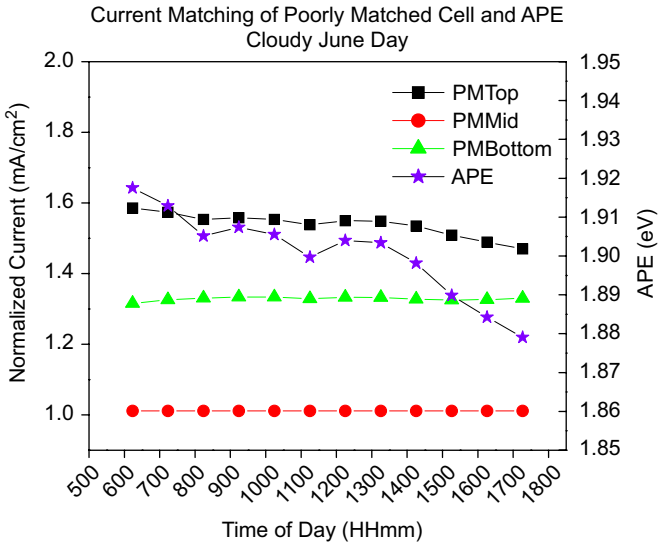

Fig. 6. Poorly matched cell's sub-cell currents and APE vs. time of day on the cloudy June day.

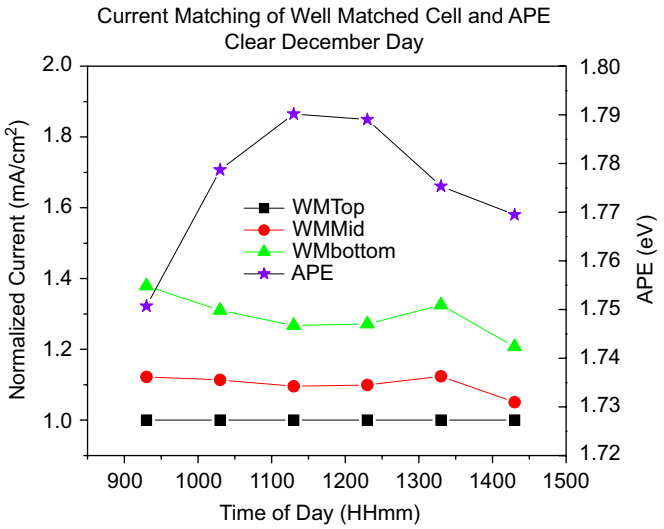

Fig. 7. Well-matched cell's sub-cell currents and APE vs. time of day on the clear December day.

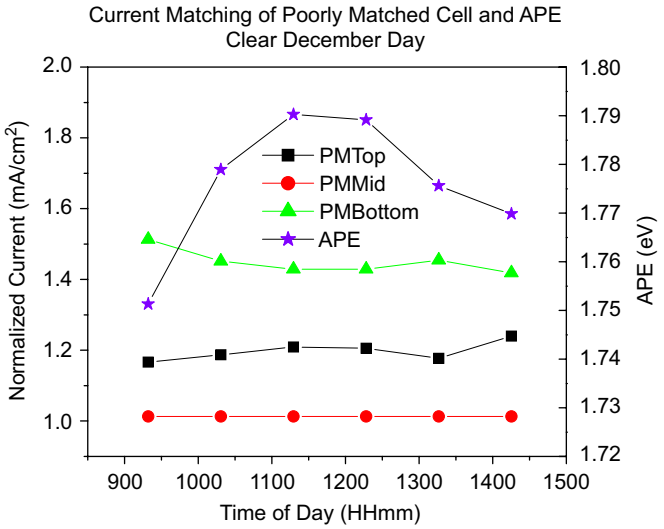

Fig. 8. Poorly matched cell's sub-cell currents and APE vs. time of day on the clear December day.

AM1.5 APE of 1.88 eV. At the start and end of the day, the APE was at its highest value, indicating that a lot of blue light was present. Because of this, the top sub-cell of both cells had its highest output at these times. It followed the trend of the APE curve. The bottom sub-cell of both cells approximately followed the inverse shape. In the well-matched cell, the top-cell current was on average 14% higher than the current-limiting cell. The bottom and middle cells were well matched, with an average current difference of 3%. The high photon energy of an APE of 1.89 eV was mainly absorbed by the top cell and so it had the highest current. Less red and green light was available for the other two cells. For the poorly matched cell a similar general shape is observed as for the well-matched cell but the current differences were larger. The top-cell current was, on average, 50% higher than the middle-cell current and the bottom-cell current was 27% higher. Because the APE was so close to the AM1.5 APE, the matching was also very close to the reference conditions.

The cloudy June day results for both cells are shown in Figs. 5 and 6. The day's APE on the cloudy day was the same as that on the clear day, i.e., 1.89 eV, but it showed a generally decreasing trend. Sky images of that day showed the cloud cover to slowly decrease as the day progressed [17]. This reduced the scattering of blue light slightly and allowed a bit more red light to reach the Earth surface. In both cells, the top cell's output followed a similar trend as the APE curve, generally rising and falling with it. The bottom cell's output rose slightly over the course of the day as the APE decreased. The slightly longer wavelengths towards the end of the day contributed to its improving performance. When compared with performance on the clear June day, it is seen that cell behaviour on both days was very similar. The middle cell was always the current-limiting cell. In the well-matched cell, its current was an average of 17% and 6% lower than in the top and bottom cells, respectively. In the poorly matched cell, its current was an average of 53% and 32% lower than in the top and bottom cells, respectively.

Please cite this article as: P. Krishnan, et al., Sol. Energy Mater. Sol. Cells (2008), doi:10.1016/j.solmat.2008.09.031

Comparing the two cells and 2 days, the clear June day provided the best matching on both cells. It was the closest in performance to AM1.5 conditions. On the clear day, the shape of the APE was more constant than on the cloudy day (compare Figs. 4 and 5). This relatively constant shape kept the matching between the cells constant for a large portion of the day. The variance of the well-matched cell's bottom sub-cell current can be considered as an example. Ignoring the two readings at the beginning and end of the clear June day (when the APE was higher than most of the day), the standard deviation of the mean of the remaining points was 3.09×10^{-3} mA/cm^2. On the cloudy day, the incident light changed slightly but significantly enough to constantly change the output of the cells. The standard deviation of the same bottom-cell output throughout this day was 4.23×10^{-3} mA/cm^2, higher by about a factor of 1.4. A similar result was found when comparing poorly matched cell bottom sub-cell currents. Current deviations differing by one order of magnitude were found when comparing the top sub-cells. This could explain why the average current matching on the cloudy day was slightly worse than the clear day although both days had an overall APE of 1.89 eV. The current varied more on the cloudy day with changing APE shape and therefore the matching suffered.

3.2. December days

The clear December day results are shown in Figs. 7 and 8. In the morning, the APE was at its lowest with a value of about 1.75 eV. As the day passed, the APE rose slightly to reach a maximum of just over 1.79 eV. Overall, the day's APE was 1.78 eV—5.3% lower than the reference APE. In both cells, the bottom cell produced the highest current because of the redder winter spectrum. The longer light path scattered more blue light, leaving the red light behind for the bottom cell to absorb. Generally, the top cell followed the APE trend, while the middle and bottom cells were approximately inversely related to the APE curve. In the well-matched cell, the top cell was the current-limiting cell because of the relative lack of blue light. Although the current-limiting cells were different compared to the reference matching condition, the difference between the top and middle cells was almost identical, approximately 10–11%. It was expected that the bottom cell would have the highest output and this was confirmed. The bottom-cell current was on average 29% higher than the top-cell current. In the poorly matched cell, the top and bottom cells had currents on average 19% and 44% higher than in the middle cell, respectively. The middle cell was clearly the current-limiting cell, unlike the well-matched cell for which the top cell was limited.

To understand why the current-limiting cell changed between the triple cells, the spectral response can be examined. The spectral response of both cells is shown in Fig. 9. The top sub-cell of the poorly matched cell (PMTop) had a wider response than that of the well-matched cell (WMTop). The integrated current density over the same range of wavelengths was therefore higher. The middle sub-cell of the poorly matched cell (PMMid) had a smaller response than the corresponding well-matched sub-cell (WMMid). Its integrated current density over the same range of wavelengths was lower. Combining these effects explains why the top sub-cell of the well-matched cell and the middle sub-cell of the poorly matched cell were current limiting for the same irradiance.

Overall, on this day, it can be seen that the matching of both cells was less than ideal. Compared to the reference matching, the top and middle cells were closer in current but the middle- and bottom-cell difference grew. This was the effect of a redder

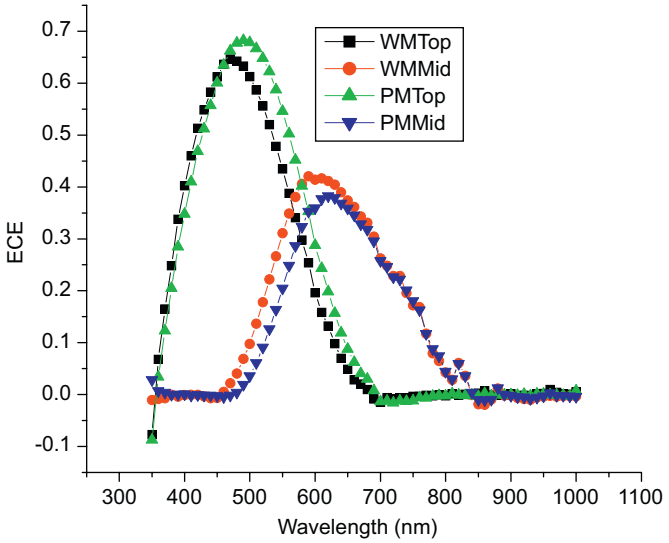

Fig. 9. Spectral response of top and middle sub-cells of both triple cells.

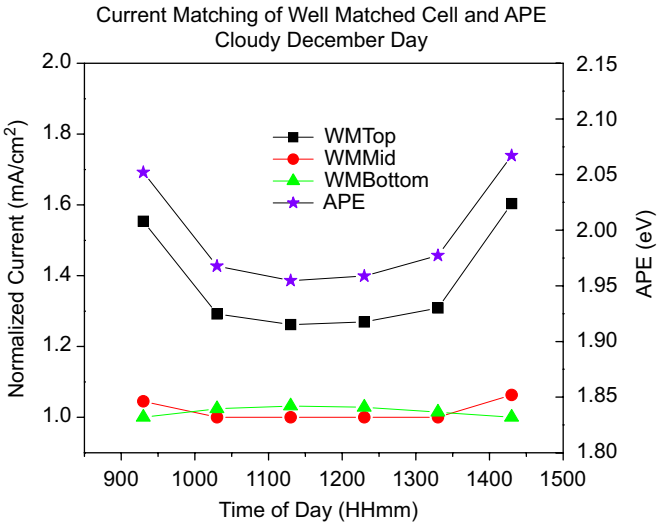

Fig. 10. Well-matched cell's sub-cell currents and APE vs. time of day on the cloudy December day.

spectrum, which allowed the bottom cell to produce more current. The change in APE from the June to December days underlines the challenges in matching cells for different conditions.

The cloudy December day results are seen in Figs. 10 and 11. The APE of 1.99 eV on this day was the highest of all the 4 days and 5.5% higher than the AM1.5 APE. The longer winter sunlight path causes high scattering of blue light. This scattering was increased due to the cloud cover during most of the day. These two factors contributed to a large amount of diffuse blue light reaching the Earth. There was high scattering due to the low sun angle during the ends of the day. As the sun rose, the angle-induced scattering reduced but the cloud-induced scattering persisted. Thus, the APE showed a parabolic trend for the day. During the morning and evening hours the middle cell had a higher current than the bottom cell. A higher fraction of blue–green light allowed it to produce a current 5% higher, on average, than that of the bottom cell. During the middle of the day when angle-induced scattering reduced and the portion of red light increased, the bottom-cell output rose to about 3% above that of the middle cell. The

Please cite this article as: P. Krishnan, et al., Sol. Energy Mater. Sol. Cells (2008), doi:10.1016/j.solmat.2008.09.031

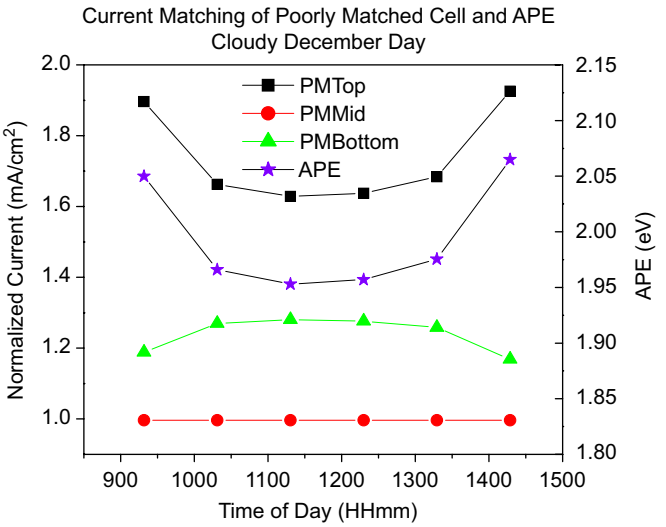

Fig. 11. Poorly matched cell's sub-cell currents and APE vs. time of day on the cloudy December day.

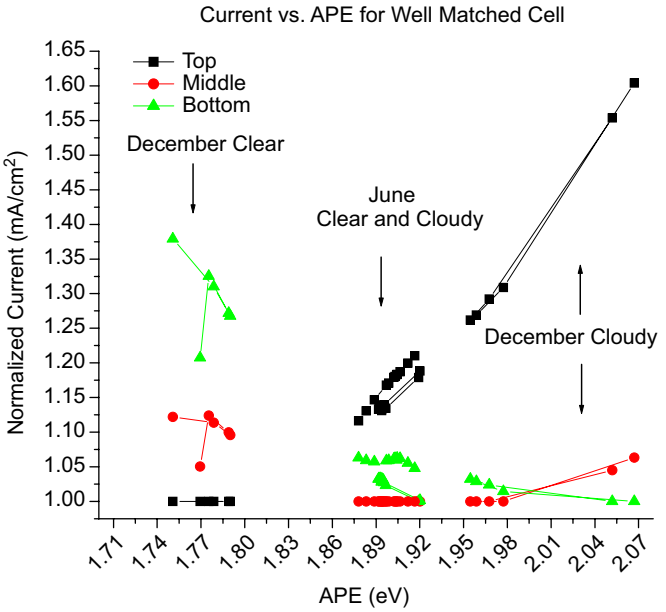

Fig. 12. Behaviour of sub-cell currents vs. APE of the well-matched cell for each of the 4 days studied.

matching between the middle and bottom cells was ideal. Because of the high APE, the top cell produced the highest output at all times, tracking the APE shape. Relative to the current-limiting cell, the top-cell output was an average of 38% higher. Thus, the top cell was not as well matched with the other two sub-cells on this day compared to the June days. Its average output difference compared to the current-limiting cell was more than double that of the June days and more than triple that of the reference mismatch of 11%. In the poorly matched cell, the matching was particularly bad during the morning and evening hours. The top-cell current was much larger than that of the current-limiting middle cell. The current matching improved slightly during the afternoon. The top and bottom sub-cells had average outputs of 75% and 25% higher than that of the middle cell, respectively. When compared with the other days and reference conditions, the

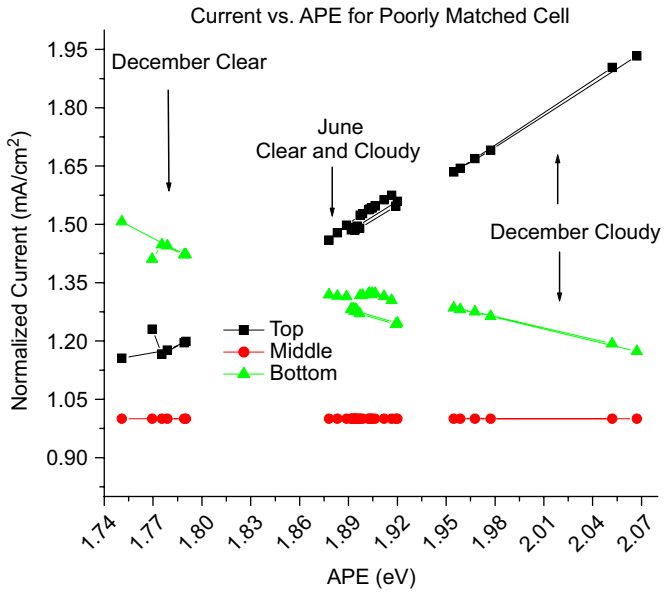

Fig. 13. Behaviour of sub-cell currents vs. APE of the poorly matched cell for each of the 4 days studied.

Table 3
Relative currents versus each day's APE for well-matched and poorly matched cells

Day	APE	Well-matched cell			Poorly matched cell		
		Top	Middle	Bottom	Top	Middle	Bottom
Clear June	1.89	1.14	1	1.03	1.50	1	1.27
Cloudy June	1.89	1.17	1	1.06	1.53	1	1.32
Clear December	1.78	1	1.10	1.29	1.19	1	1.44
Cloudy December	1.99	1.38	1	1.02	1.75	1	1.25

matching was very poor. The constantly changing APE caused by clouds and winter irradiance provided very unstable performance. It caused drastically different outputs even in the well-matched cell.

3.3. Summary

Figs. 12 and 13 summarize the normalized current data vs. APE for each cell, while Table 3 shows the relative currents for well-matched and poorly matched cells, compared to the averaged daily APE, as discussed in detail above. It is evident that as the APE increased, the top-cell current rose consistently. The opposite happened for the bottom-cell currents—they decreased as APE increased. For all of the days, the middle cells were near the bottom of the graph as they are the current-limiting cells, except for the early morning and late afternoon of the cloudy winter day, when bottom and middle cells exchanged their role as current-limiting cell. These figures, in combination with Table 3, confirm the results of the individual day observations. The main conclusion is that as the APE deviates from the value that the cells are tuned to, the AM1.5 standard value of 1.88 eV, the current matching deteriorates.

4. Conclusion

The current matching of two triple cells has been studied for 4 days representative of the Dutch climate. Overall, it was found that small changes in the spectrum upset the matching greatly.

Please cite this article as: P. Krishnan, et al., Sol. Energy Mater. Sol. Cells (2008), doi:10.1016/j.solmat.2008.09.031

This is an important aspect of triple cells that must be studied further and improved upon. It must be accepted that it is very difficult to tune the cells to be matched under all spectral conditions. To maximize cell output the long-term Dutch spectrum (over decades) must be examined. The cell should be designed to provide the best matching under the times of the year when incident energy is highest.

Acknowledgements

We would like to thank Alexander Los and Wouter Knap from KNMI for providing the irradiation data for this project.

References

[1] D.L. King, J.A. Kratochvil, W.E. Boyson, Measuring solar spectral and angle-of-incidence effects on photovoltaic modules and solar irradiance sensors, in: Conference Record of the 26th IEEE Photovoltaic Specialists Conference, Anaheim, CA, USA, 1997, pp. 1113–1116.
[2] S. Nann, K. Emery, Spectral effects on PV-device rating, Sol. Energy Mater. Sol. Cells 27 (1992) 189–216.
[3] Y. Hirata, T. Tani, Output variation of photovoltaic modules with environmental factors—I. The effect of spectral solar radiation on photovoltaic module output, Sol. Energy 55 (1995) 463–468.
[4] Y. Hirata, T. Inasaka, T. Tani, Output variation of photovoltaic modules with environmental factors—II. Seasonal variation, Sol. Energy 63 (1998) 185–189.
[5] T. Minemoto, M. Toda, S. Nagae, M. Gotoh, A. Nakajima, K. Yamamoto, H. Takakura, Y. Hamakawa, Effect of spectral irradiance distribution on the outdoor performance of amorphous Si/thin-film crystalline Si stacked photovoltaic modules, Sol. Energy Mater. Sol. Cells 91 (2007) 120–122.
[6] D. Berman, D. Faiman, B. Farhi, Sinusoidal spectral correction for high precision outdoor module characterization, Sol. Energy Mater. Sol. Cells 58 (1999) 253–264.
[7] R. Gottschalg, D.G. Infield, M.J. Kearney, Experimental study of variations of the solar spectrum of relevance to thin film solar cells, Sol. Energy Mater. Sol. Cells 79 (2003) 527–537.
[8] S. Nann, C. Riordan, Solar spectral irradiance under clear and cloudy skies: measurements and a semiempirical model, J. Appl. Meteorol. 30 (1991) 447–462.
[9] R.H. Franken, R.L. Stolk, H. Li, C.H.M. van der Werf, J.K. Rath, R.E.I. Schropp, Understanding light trapping by light scattering textured back reflectors in thin-film n–i–p-type silicon solar cells, J. Appl. Phys. 102 (2007) 014503.
[10] W.G.J.H.M. vanSark, Simulating performance of solar cells with spectral downshifting layers, Thin Solid Films 516 (2008) 6806–6812.
[11] R.E. Bird, C. Riordan, Simple solar spectral model for direct and diffuse irradiance on horizontal and tilted planes at the Earth's surface for cloudless atmospheres, J. Clim. Appl. Meteorol. 25 (1986) 87–97.
[12] D.R. Myers, private communication, 2006.
[13] Baseline Surface Radiation Network (BSRN), 〈http://bsrn.ethz.ch/〉.
[14] ASTM, Standard Tables for Reference Solar Spectral Irradiances: Direct Normal and Hemispherical on 37° Tilted Surface, Standard G173-03e1, 2003.
[15] B. Houshyani Hassanzadeh, A. Los, A.C. de Keizer, W. Knap, W.G.J.H.M. van Sark, The effect of varying solar spectrum on the energy performance of solar cells, in: G. Willeke, H. Ossenbrink, P. Helm (Eds.), Proceedings of the 22nd European Photovoltaic Solar Energy Conference, WIP-Renewable Energies, Munich, Germany, 2007, pp. 2652–2658.
[16] B. Houshyani Hassanzadeh, A.C. de Keizer, N.H. Reich, W.G.J.H.M. van Sark, The effect of varying solar spectrum on the energy performance of solar cells, in: Proceedings of the 22nd European Photovoltaic Solar Energy Conference, (Eds. G. Willeke, H. Ossenbrink, P. Helm) WIP-Renewable Energies, Munich, Germany, 2007, 2652–2658.
[17] B. Houshyani Hassanzadeh, The effect of a varying solar spectrum on solar cells energy performance, M.Sc. Thesis, Utrecht University, 2006.

Please cite this article as: P. Krishnan, et al., Sol. Energy Mater. Sol. Cells (2008), doi:10.1016/j.solmat.2008.09.031